Efficient and robust collective excitation transfer in a multimode quantum memory using modulated adiabatic pulses

Ao-Lin Guo,[1,2] Tao Tu [1,2,*] Guang-Can Guo,[1] and Chuan-Feng Li[1,†]

[1]*Key Laboratory of Quantum Information, University of Science and Technology of China, Chinese Academy of Sciences, Hefei 230026, People's Republic of China*
[2]*Department of Physics and Astronomy, University of California at Los Angeles, California 90095, USA*

Quantum memories are building blocks for a variety of quantum technologies. However, the collective transfer between optical excitations and spin-wave excitations determines the performance of the quantum memory. Here we propose a method for collective excitations transfer with high efficiency and fidelity in a multimode quantum memory. The pulse uses modulations of the control parameters to cancel the nonadiabatic transitions during the evolution. We demonstrate the universality of the control pulse by simulations for an atomic frequency comb spin-wave quantum memory. The protocol is robust to various experimental imperfections in the pulse amplitude and duration. The protocol also allows one to achieve high multiplexed storage at small cost on efficiency reduction. The protocol is particularly useful in retaining the phase coherence since the environment dissipation would decohere the system. These results pave a way for efficient and robust coherent manipulations in a multiplexed quantum memory.

I. INTRODUCTION

Quantum memories are essential elements in various quantum information tasks: constituting repeaters for long-distance quantum communication and enabling functional nodes for distributed quantum computation [1–6]. The implementation of quantum memories exploits the storage and manipulation of photons (flying qubits) and matter (stationary qubits). A large variety of physical systems are currently being demonstrated as platforms for quantum memories such as atomic ensembles [7], single atoms in cavities [8], nitrogen-vacancy centers [9], and spins in quantum dots [10,11]. Among them, rare-earth ions doped in solids are a promising candidate [12]. They can provide strong light-matter interactions through high number densities, while also offering perspectives for integration and scalability with existing solid-state technology. Impressive progress has been realized in this system, including excellent coherence properties about hours timescales [13], storage of entanglement [14,15], polarization [16–18], and orbital angular momentum of photons [19].

There are numerous performance metrics for quantum memories including high efficiency, high fidelity, large multimode capacity, on-demand readout, and long storage time [1,3]. However, finding a scheme that simultaneously fulfills all these good properties is challenging. The atomic frequency comb–spin-wave (AFC-SW) protocol has been proposed as a useful resource which combines several figures of merit [20–23]. Since rare-earth ions doped in crystals exhibit large inhomogeneous broadening of the optical transitions, the AFC-SW protocol can tailor this feature to enable temporal or frequency multiplexed quantum storage [24–26]. Furthermore, the ability to read out the stored states on demand can be achieved by applying control pulses to transfer the optical atomic excitations to collective spin excitations (spin wave). This transfer also provides a much longer storage time due to the long-lived spin excitations. While the AFC-SW protocol offers these advantages, the inevitable imperfections in the control pulses can lead to a serious reduction in overall efficiency and fidelity. In the current experiments, chirped adiabatic pulses are commonly used where transfer efficiency has a limited value of 67% [22]. In addition, the total duration of the input pulses includes the train of signal modes and the control pulse. Therefore, with longer control pulses, the multimode capacity of the memory is reduced more. Operating a solid-state spin-wave quantum memory with simultaneously excellent efficiency and fidelity and multiplexing has so far remained elusive, because of the limitations of control pulses.

In this paper, we propose a scheme to design the control pulses for collective excitations transfer with high efficiency and fidelity, which also work with multimode storage. We use a modulated adiabatic pulse approach, in which the control parameters of the pulse are tailored to compensate undesired nonadiabatic transitions. Several strategies have been put forward to design an adiabatic pulse [27], while they are challenging to apply in the spin-wave quantum memories. Among these strategies, an auxiliary control field is introduced which requires complex experimental resources [28–31], composite pulse sequences are utilized which are at the price of a very fast growth in the number of pulses [32,33], or the pulse is only applied to multistate transfer such as three-level systems [34–36]. Moreover, as many existing protocols generally assume ideal evolution, their robustness to
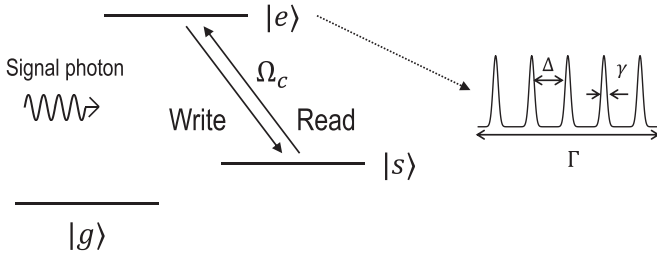
---

*tutao@ustc.edu.cn
†cfli@ustc.edu.cn

FIG. 1. Schematic diagram of optical quantum memory based on the AFC-SW protocol. The signal photon field is absorbed by the ensemble with atomic frequency comb. A pair of control pulses transfer the atomic excitations forth into and back from the spin excitations for on-demand readout and long-term storage.

experimental variations and environment dissipation remains an open question. Here we develop the modulated adiabatic pulse relevant to spin-wave quantum memories, and address its robustness both to pulse imperfections and environment dissipation.

In Sec. II we describe the AFC-SW protocol and focus on the collective excitations transfer process from the optical transition to the spin transition. In Sec. III, we present a control model taking into account the main pulse deviations and environment noise sources. Then we use the idea of a modulated adiabatic pulse to design driving amplitude, duration, and frequency detuning of the control pulses. In Sec. IV, we give intensive simulations of the control pulses with relevance to applications in a AFC-SW based quantum memory. As our numerical simulations show, the modulated adiabatic pulse can realize the desired excitations transfer with a high efficiency even under realistic situations and outperform the chirped adiabatic pulse available so far. More importantly, the designed pulses are robust to pulse imperfections and dissipation effects of environment. In Sec. V, we also show the modulated pulse can preserve the phase coherence which is at the heart of the collective excitations in a spin-wave quantum memory. We provide conclusions and an outlook for future works in Sec. VI.

II. CONTROL PULSES IN THE AFC-SW PROTOCOL

The AFC-SW protocol uses the unique systems of rare-earth ions doped in crystals such as Pr^{3+}:Y_2SO_5 [22] or Eu^{3+}:Y_2SO_5 [21]. The memory is an ensemble of atoms with three levels as shown in Fig. 1. The optical transitions line between levels $|g\rangle$ and $|e\rangle$ is inhomogeneously broadened and is spectral tailored into a comb-shaped structure, where narrow peaks with a width γ and a periodicity Δ span a large frequency range Γ. The input signal photon resonant with the atomic frequency comb can be mapped onto an optical atomic excitation. This collective excitation is described as a single atomic excitation delocalized over all the atoms in the solid [20]:

$$\sum_{j=1}^{N} e^{-i\Delta_j t} e^{-ik_s z_j} |g_1 \cdots e_j \cdots g_N\rangle. \qquad (1)$$

Here, j denotes the jth atom in the solid, k_s is the wave number of the absorbed signal photon field, and Δ_j and z_j are the

frequency detuning and the position of the atom, respectively. After a time $2\pi/\Delta$, the collective excitations rephase giving rise to a photon reemission. This AFC based scheme only stores the photon states as collective atomic excitations with fixed storage time. Before the collective emission, one can apply a control pulse to transfer the optical excitation forth into a long-lived spin state $|s\rangle$. This collective spin excitation is described as

$$\sum_{j=1}^{N} e^{-i\Delta_j(2\pi/\Delta - T_0)} e^{-i(k_s - k_c)z_j} |g_1 \cdots s_j \cdots g_N\rangle. \qquad (2)$$

Here, $2\pi/\Delta - T_0$ is the delay between the control pulse and the signal photon field and k_c is the wave number of the control pulse. After a spin-wave storage time T_s, a second control pulse is applied to transfer the excitation back from the spin wave. In this context, the full AFC-SW protocol achieves on-demand storage and retrieval and long-term storage.

III. MODULATED ADIABATIC PULSES

We consider an ensemble of three-level atoms and a pair of control pulses which are applied to transfer collective excitations between the $|e\rangle$ and $|s\rangle$ levels. We use the semiclassical picture where the collective atomic state is treated as a tensor product of single-atom states. In practice, the control pulse is implemented as a shape of

$$\Omega(t)\cos[\omega_c(t)t - k_c z] \qquad (3)$$

with the time-dependent driving amplitude $\Omega(t)$ and the frequency $\omega_c(t)$. Since the cross section of the control pulse is bigger than the sample, we can assume that the atom-pulse interaction is uniform for all of the atoms in the crystal. Working in the rotating wave approximation, the Hamiltonian of the control pulse is modeled as

$$H_0(t) = \frac{\Omega(t)}{2}\sigma_x + \frac{\Delta(t)}{2}\sigma_z, \qquad (4)$$

where σ_i are the Pauli operators defined in the subspace of $|e\rangle$ and $|s\rangle$, and $\Delta(t)$ is the frequency detuning of the control pulse with respect to the atomic resonance between the $|e\rangle$ and $|s\rangle$ levels.

In current experiments, chirped adiabatic pulse has been proposed [37] and demonstrated to facilitate the excitations transfer in the AFC-SW memory [21,22]. As shown in Fig. 2(a), this type of control pulse has a hyperbolic secant temporal profile and is spectrally chirped as a hyperbolic tangent,

$$\Omega(t) = \Omega_{\max}\text{sech}(t/\tau_c), \qquad (5)$$

$$\Delta(t) = \frac{\Gamma}{2}\tanh(t/\tau_c). \qquad (6)$$

Here $\Omega_{\max}$ is the maximum amplitude of the pulse, the variation range of $\Delta(t)$ covers the atomic frequency comb range Γ, and τ_c determines the time of the adiabatic sweep. This shape is considered adiabatic in the large τ_c limit, as the driving amplitude and the frequency chirp vary slowly in time. Although this kind of control pulse is relatively easy to implement, its effectiveness is limited when environment decoherence and pulse fluctuations occur in experiments.
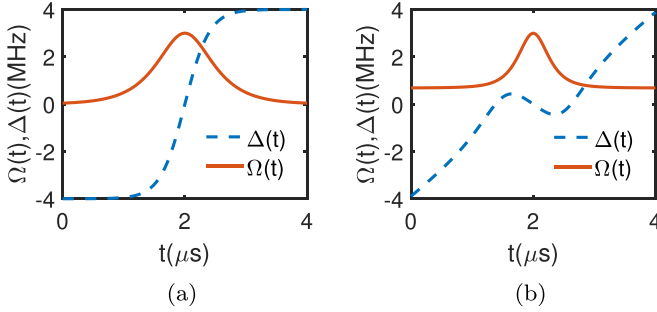
FIG. 2. Examples of the chirped adiabatic pulse (a) and the modulated linear pulse (b). The maximum amplitude $\Omega_{\max}$, the duration T_0, and the frequency range Γ specify the control pulses for a particular implementation. Here $\Omega_{\max} = 3$ MHz, $T_0 = 4$ μs, and $\Gamma = 8$ MHz.

To address this drawback, we use the approach of modulated adiabatic pulse to design the control field to realize fast control time while maintaining the high efficiency of the adiabatic evolution. For a time-dependent Hamiltonian H_0 in Eq. (4), the nonadiabatic evolution part can be described as

$$H_{na} = \frac{i}{2} \sum_{n=1,2} (|n\rangle\langle\partial_t n| - |\partial_t n\rangle\langle n|), \qquad (7)$$

where $|n\rangle$ denotes the instantaneous eigenstates of the original Hamiltonian H_0, and $|\partial_t n\rangle$ is the derivative of the instantaneous eigenstates with respect to time. In general, one can construct an additional interaction term $H_{ca} = -H_{na}$ to cancel the effect of the nonadiabatic evolution part. Thus, the total Hamiltonian $H_t = H_0 + H_{ca}$ allows the system evolution to follow the adiabatic eigenstates of the original Hamiltonian H_0 without transitions between these adiabatic eigenstates. For the control field of H_0 in Eq. (4), one can use an explicit form of the auxiliary field

$$H_{ca} = \tfrac{1}{2}\partial_t\phi\sigma_y \qquad (8)$$

with the angle $\phi = \arctan(\frac{\Omega(t)}{\Delta(t)})$.

Schemes to introduce an auxiliary control field H_{ca} have been presented in various platforms [28–31]. However, these schemes require an additional laser or microwave field and a careful design to realize the interaction term absent in the original Hamiltonian H_0. To avoid the demanding requirements for complex experimental resources, we use a modulation of parameters in the original control pulse to achieve the effect of this extra interaction field H_{ca}.

Starting from an original control Hamiltonian $H_0(t) = \frac{\Omega(t)}{2}\sigma_x + \frac{\Delta(t)}{2}\sigma_z$, we modulate the control parameters $\Omega(t)$ and $\Delta(t)$ in such a form $H_{ma}(t) = \frac{\Omega_{ma}(t)}{2}\sigma_x + \frac{\Delta_{ma}(t)}{2}\sigma_z$ to achieve the same effect as the total Hamiltonian $H_0(t) + H_{ca}(t) = \frac{\Omega(t)}{2}\sigma_x + \frac{\Delta(t)}{2}\sigma_z + \frac{1}{2}\partial_t\phi\sigma_y$. In this way, we absorb the auxiliary term $H_{ca} = \frac{1}{2}\partial_t\phi\sigma_y$ into the modulation form of the original Hamiltonian H_0 using the transformations of Pauli matrices.

Usually, there is a major class of control pulses for implementation of the Hamiltonian H_0 in Eq. (4): linear sweeping pulse (Landau-Zener model) [38],

$$\Omega(t) = \Omega_0, \qquad (9)$$

$$\Delta(t) = vt, \qquad (10)$$

where v is the sweeping rate. We present our protocol that modulates and corrects existing control pulses. For the original linear sweeping pulses, we can modulate their parameters as

$$\Omega_{ma}(t) = \Omega_0 \sqrt{1 + \frac{\left(\Omega_0\frac{d\Delta}{dt}\right)^2}{4\Omega_0^2\left[\Omega_0^2 + \Delta(t)^2\right]^2}}, \qquad (11)$$

$$\Delta_{ma}(t) = \Delta(t) - \frac{1}{2}\frac{d}{dt}\left[\arctan\left(\frac{-\Omega_0\frac{d\Delta}{dt}}{2\Omega_0\left[\Omega_0^2 + \Delta(t)^2\right]}\right)\right]. \qquad (12)$$

The shapes of the modulated linear pulse are illustrated in Fig. 2(b). For quantum memory applications, the following simulations of these pulses use the realistic values of control parameters from experiments, including pulse maximum amplitude $\Omega_{\max}$, duration T_0, and frequency range Γ [21,22]. We note that here we consider the case of linear sweeping pulse, while the protocol of modulated pulses is independent of the physical case under consideration.

The master equation of the system is given by

$$\dot{\rho} = -i[H, \rho] + \sum_k \Gamma_k L_k[D], \qquad (13)$$

where H is the control Hamiltonian and $L_k[D] = D\rho D^+ - \frac{1}{2}D^+D\rho - \frac{1}{2}\rho D^+D$ is the Lindblad operator for the dissipative process. Here we consider the relaxation process from the excited state $|e\rangle$ to the spin state $|s\rangle$ at a rate $\Gamma_1 = 6.6$ kHz, and the dephasing process of the excited state $|e\rangle$ at a rate $\Gamma_2 = 30.5$ kHz. The spin state dephasing does not play a significant role during the timescale of the control process. In addition, we include the spectral diffusion of the excited state $|e\rangle$ as a fluctuation around the detuning $\Delta + \delta\Delta$. This fluctuation is modeled as a Gaussian distribution with a standard deviation $\sigma_{sd} = 2\pi \times 31$ kHz. These realistic values are extracted from the measurements of time-resolved optical properties in rare-earth ions doped in crystals [39]. After sampling a random value of this noise $\delta\Delta$, we numerically calculate the master equation. The time evolution of the system is averaged over many repetitions of the simulations.

IV. PERFORMANCE EVALUATION OF CONTROL PULSES

A. Efficiency

There are a number of evaluation criteria for assessing quantum memory performance, with efficiency and fidelity being two of the most important [1,3]. Efficiency is defined as the probability to recover a stored photon, and fidelity is defined as the overlap between the recovered state and the input state. The current experiments show that efficiency is the main limiting factor [22,23], and the increase of entanglement rate in quantum networks depends crucially on the memory efficiency, therefore we discuss the efficiency metric in this section first, and then the fidelity metric in the next section.
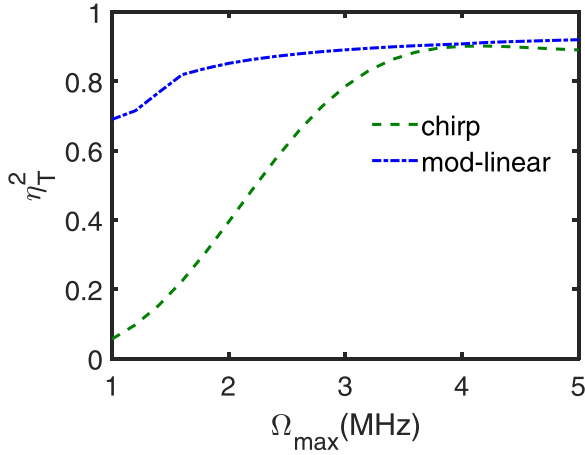
FIG. 3. Excitation transfer efficiency of the modulated linear pulse and the chirped adiabatic pulse as a function of the maximum driving strength Ω_{max} for a constant pulse duration $T_0 = 6$ μs and a frequency range $\Gamma = 8$ MHz.

FIG. 4. The converted populations during the control pulses: the chirped adiabatic pulse (a) and the modulated linear pulse (b) for $\Omega_{max} = 3$ MHz and $\Gamma = 8$ MHz, highlighting the adiabatic evolution of modulated pulses. P_e and P_s denote the populations of the excited and ground states, respectively.

The efficiency of the AFC-SW memory protocol is given by $\eta = \eta_{AFC}\eta_T^2\eta_{SW}$. Here η_{AFC} is the efficiency of the absorption and reemission of the atomic frequency comb, η_{SW} accounts for the efficiency loss due to the decoherence effect during the spin-wave storage, η_T is the transfer efficiency of one control pulse, and the power index 2 includes the transfer forth and back. η_{AFC} depends on the optical depth and comb finesse and the direction of recall [20]. In the forward direction, the reabsorption effect of the photon limits the efficiency below 1. It has a formula $\eta_{AFC} = d^2 \exp(-d)\eta_{deph}$, where d is the optical depth of the sample, and η_{deph} is a dephasing factor that accounts for the finite width and shape of the AFC. In backward recall, an interference effect makes the efficiency η_{AFC} possible to reach a high value for a long sample. It has a formula $\eta_{AFC} = [1 - \exp(-d)]^2\eta_{deph}$. In the following we focus on the transfer efficiency performance η_T of various control pulses.

We begin by investigating the transfer efficiency of our modulated protocol as a function of the maximum amplitude Ω_{max} of the control pulses. After initializing excitations into $|e\rangle$ level, a pair of control pulses is applied to transfer the excitations into $|s\rangle$ level, and back and forth. In Fig. 3, for a typical pulse duration $T_0 = 6$ μs and a frequency range $\Gamma = 8$ MHz, we vary maximum strength Ω_{max} to explore different regimes of the control pulses. The presence of various environment dissipation effects preclude the perfect transfer efficiency expected in their absence. However, the transfer efficiency of the modulated linear pulse under the realistic implementations, significantly outperforms that of the chirped adiabatic pulse. Furthermore, experimental realization of a quantum memory in the single-photon regime is challenging since the strong control pulses create noise which severely dominates the weak signal mode. The modulated adiabatic protocol achieves enhancement of seven times in the transfer efficiency over the chirped adiabatic protocol when the driving amplitude Ω_{max} decreases to 1 MHz. The modulated pulses require a relatively small control field to realize a high efficiency, and thus allow one to reduce the resulting noise
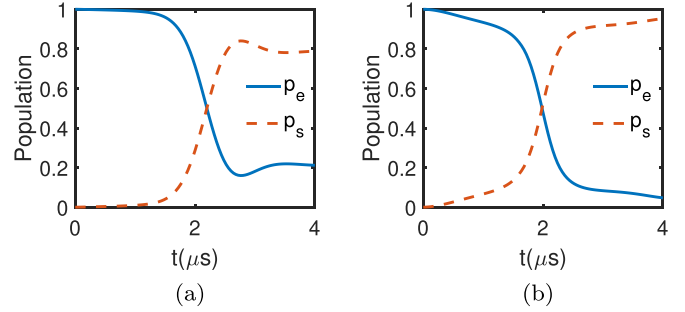
and increase the signal-to-noise ratio of the memory at the single-photon level.

To highlight the dynamics of different protocols, in Fig. 4, we show the time-resolved population during the modulated pulse and the chirped adiabatic pulse for a constant pulse amplitude $\Omega_{max} = 3$ MHz and a frequency range $\Gamma = 8$ MHz. The change in population occurs mainly in the center of the process for the chirped adiabatic pulse; however, this change is continuous over time for the modulated protocol. This evolution is a signature of the adiabatic evolution of modulated pulses: the system stays in the instantaneous adiabatic state at all times without sudden transitions between the adiabatic states. Moreover, we find that the maximal population of the $|s\rangle$ state for the modulated pulse is larger than the chirped adiabatic pulse, consistent with their theoretical expectation.

To characterize the speedup of our modulated scheme, we turn to simulate the transfer efficiency by varying the length T_0 of the control pulses. As shown in Fig. 5 for a typical pulse amplitude $\Omega_{max} = 3.5$ MHz and a frequency range $\Gamma = 8$ MHz, the modulated linear pulse maintains high transfer efficiency when the total duration is reduced. For example, at the pulse length $T_0 = 2$ μs, the modulated pulses can
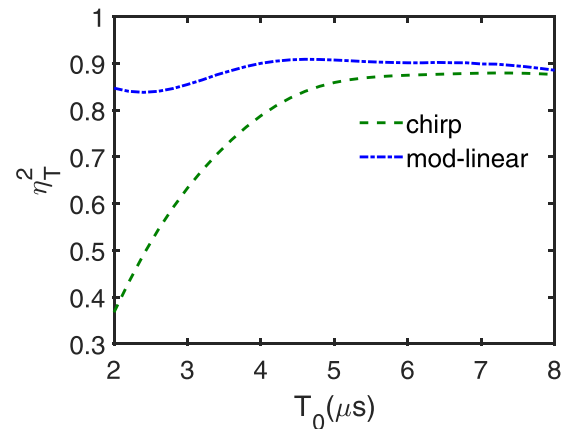

FIG. 5. Excitation transfer efficiency as a function of the pulse duration T_0 for the modulated linear pulse versus the chirped adiabatic pulse. Here the driving strength and the frequency range are constants $\Omega_{max} = 3.5$ MHz and $\Gamma = 8$ MHz.
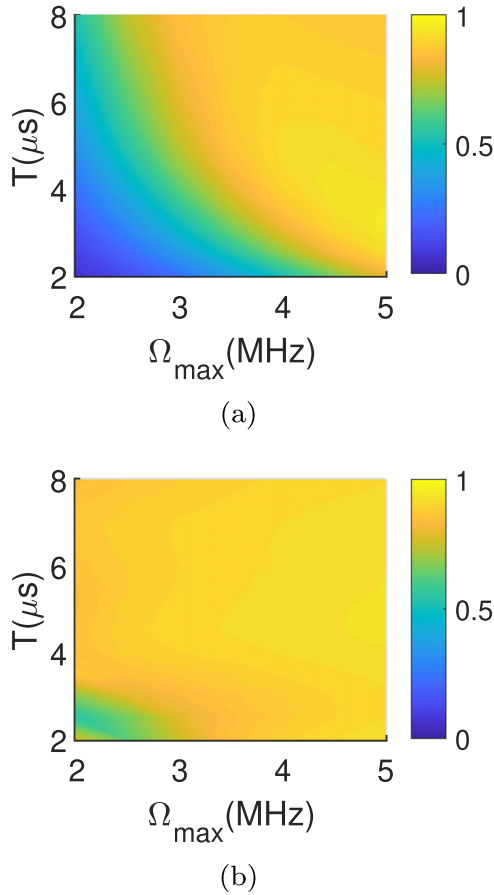
(a)

(b)

FIG. 7. (a) The lines display the transfer efficiency as a function of the spectral diffusion width σ_{sd}, representing robustness of different control protocols to the dissipation effects. Here $\Omega_{max} = 3.5$ MHz, $T_0 = 5$ μs, and $\Gamma = 8$ MHz. (b) The number of modes that can be stored as a function of the pulse duration T_0 for a typical range of atomic frequency comb $\Gamma = 8$ MHz. The multimode capacity decreases for a longer pulse length, reflecting the trade-off between transfer efficiency and multiplexing ability.

(a)

(b)

FIG. 6. Two-dimensional plot of the transfer efficiency as a function of the pulse strength Ω_{max} and the pulse duration T_0 for different control protocols: (a) the chirped adiabatic pulse; (b) the modulated linear pulse. Here the frequency range is fixed at $\Gamma = 8$ MHz.

reach the efficiency of 85%, which is two times larger than that of the chirped adiabatic pulse. Two main mechanisms are responsible for the efficiency behavior of the modulated pulse in Fig. 5: the efficiency increase with the pulse length as the conditions become increasingly adiabatic until the longer pulse is significantly affected by environment decoherence. Thus, the efficiency is determined by the competition between the adiabatic evolution and the dissipation from the environment. In addition, for a short duration, the adiabatic pulse dose not satisfy the adiabatic condition well and the system dynamics would undergo a finite time oscillation [40]. Thus, as shown in Fig. 5, the efficiency would increase when T_0 becomes very small.

B. Robustness to imperfections and dissipation

To investigate the robustness to pulse imperfections of these protocols, we study the pulse shapes varying in a broad range of amplitude Ω_{max} and length T_0. In Fig. 6, we simulate the transfer efficiency with Ω_{max} and T_0 ranging from 2 to 5 MHz, and 2 to 8 μs, respectively. We find that the modulated linear pulse achieves better efficiency than the chirped adiabatic pulses for a wide range of pulse shapes. The broad range of high transfer efficiency in Fig. 6(b) demonstrates that
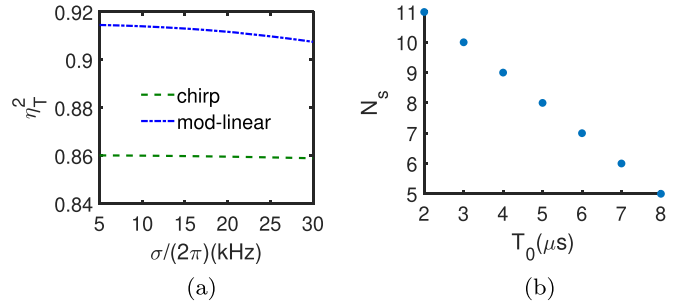
the modulated protocol is resilient to potential imperfections in real applications, such as the pulse amplitude and duration.

In realistic situations, the decrease of the efficiency probably results from the pulse shape deviations on the one hand and from the environment dissipation on the other. Since the quantum memory protocol utilizes the atomic frequency, one can anticipate that the dissipative mechanisms and fluctuations, especially the spectral diffusion of the $|e\rangle$ state, would damp the transfer between the excited state and the spin state. In Fig. 7(a), we fix the rate $\Gamma_1 = 6.6$ kHz and $\Gamma_2 = 30.5$ kHz, and present the simulation result that a decrease of the transfer efficiency is induced by an increase of the spectral diffusion width σ_{sd}. Similar to Fig. 6(b), the wide line in Fig. 7(a) suggests that the modulated pulses are also resilient to moderate dissipation from environment.

C. Multimode capacity

Another important figure of merit for quantum memories is the capacity to store multiple photons and dimensionality. The AFC-SW memory scheme can perform efficient multimode storage by using a train of input signal modes. For an atomic frequency comb range Γ, the duration of one mode that can be stored is limited as $\tau_s = 12\pi/\Gamma$. The multimode capacity stems from the fact that the comb can absorb a train of temporal modes before the first mode is reemitted after time $2\pi/\Delta$. The ratio between the duration of the train and of one mode indicates that the total number $N_s = \Gamma/6\Delta$ of the input modes can be stored. Thus, a frequency comb with many peaks (i.e., small Δ with large Γ) allows one to store a large number of temporal modes.

Now we consider the effect of the control pulses on the multimode capacity. The total duration of the write process of the quantum memory includes the train of the input signal modes and the control pulse, $T_t = N_s \tau_s + T_0$. More precisely, we consider a typical system in experiments [21,22]: an atomic frequency comb with a peak separation $\Delta = 100$ kHz spans a frequency range $\Gamma = 8$ MHz. For a total time interval $T_t = \frac{2\pi}{\Delta} = 20\pi$ μs, we compare the multimode capacity at different control pulse times in Fig. 7(b). The largest
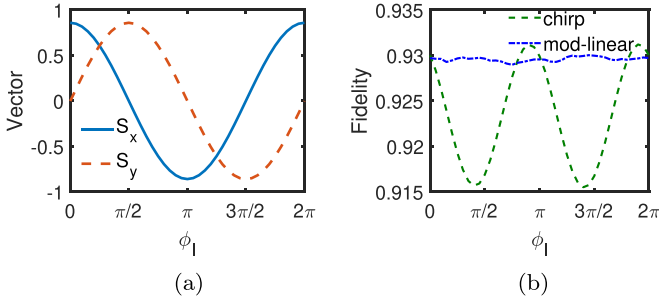
FIG. 8. Maintaining a particular phase of the transferred superposition state as the initial phase ϕ_I varies. (a) S_x and S_y components of the final state for the modulated linear pulse. (b) The transfer fidelity via different control protocols. Here $\Omega_{max} = 5$ MHz, $T_0 = 5 \, \mu s$, and $\Gamma = 8$ MHz.
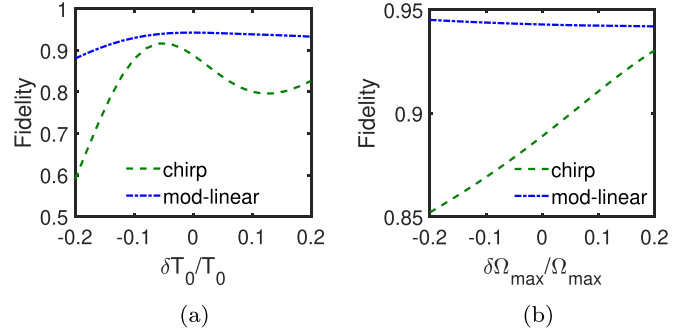

FIG. 9. Fidelity of the protocols as a function of the relative deviation of pulse strength Ω_{max} and pulse length T_0 for their fixed values: $\Omega_{max} = 3.5$ MHz and $T_0 = 4 \, \mu s$. Here $\Gamma = 8$ MHz.

number $N_s = 11$ is achieved with the duration of control pulse $T_0 = 2 \, \mu s$. Combined with Fig. 5, the efficiency (85%) of the modulated pulse with $T_0 = 2 \, \mu s$ is much better than that (36%) of the chirped adiabatic pulse with the same duration. For the chirped adiabatic pulse, the use of long control pulse duration T_0 increases the transfer efficiency. However, the price to pay is a reduction of the number of modes N_s that can be stored for a given total duration T_t. Compared with the chirped adiabatic pulse. the modulated pulse with short duration is compatible with both the transfer efficiency and the multimode capacity.

V. PRESERVING PHASE COHERENCE AND FIDELITY OF EXCITATIONS TRANSFER

Since we converse the collective optical excitations into and back from the collective spin excitations, preserving the phase coherence during the transfer protocol is crucial. The preserving of phase coherence is a measure of the fidelity of the storage process. We initialize the system in a superposition state $|\psi_I\rangle = \frac{1}{\sqrt{2}}(|s\rangle + e^{i\phi_I}|e\rangle)$, and apply the control pulse to transfer the superposition state between the excited state and the spin state. In ideal situations, the final state is expected as $|\psi_F\rangle = \frac{1}{\sqrt{2}}(|e\rangle + e^{i\phi_F}|s\rangle)$ with the same phase factor as the initial state $\phi_F = \phi_I$. In realistic situations, the phase ϕ_F would be affected by the decoherence mechanisms incorporating the dephasing and the spectral fluctuations of the excited state. For measurements of the final state, we define the density matrix of the final state as $\rho = \frac{1}{2}(S_I I + S_x \sigma_x + S_y \sigma_y + S_z \sigma_z)$, where I is the identity matrix and S_i are the corresponding components of X, Y, and Z directions. In Fig. 8(a), we show the X and Y components of the final state as a function of the initial phase. The modulated pulse achieves a cosine oscillation with the initial phase, indicating their coherent manipulations.

To quantitatively assess coherent transfer of these protocols, we use an evaluation criteria, the fidelity defined as follows:

$$F = [\text{Tr}(\sqrt{\sqrt{\rho_r}\rho_i\sqrt{\rho_r}})]^2, \quad (14)$$

where ρ_r and ρ_i are the density matrix of real and ideal target superposition states. In Fig. 8(b), we plot the fidelity for different superposition states, where the modulated pulse achieves a high fidelity beyond 93% over a wide range of initial phase ϕ_I, revealing that the modulated protocol can retain coherent transfer under the incoherent contributions from environment. We also test the sensitivity of the protocols to the perturbations in the control parameters, where we vary Ω_{max} and T_0 around their fixed values with perturbations $\delta\Omega_{max}$ and δT_0. The results are summarized in Fig. 9, which show that the modulated pulse is more robust with respect to the perturbation in the amplitude Ω_{max} or the duration T_0.

VI. CONCLUSIONS

In this work we propose modulated adiabatic pulses as a fast and robust protocol for coherent excitations transfer with applications to the quantum memories. Our approach has the flexibility to tailor the parameters to achieve the transitionless evolution in the nonadiabatic regime. Moreover, we show that the modulated protocol is more robust against experimental imperfections and environment dissipation than the chirped adiabatic pulses used so far. The protocol can be adjusted to multimode storage, without reducing its efficiency. The extension of the technique to transfer superposition states highlights its importance, since the unavoidable dissipation would affect the phase of collective excitations. Thus our protocol offers unique advantages for highly efficient and high fidelity manipulations in a multimode quantum memory. Although we exemplified it in an AFC-SW quantum memory, the technique can be applied to various quantum memory schemes and physical platforms [41–45].

[1] C. Simon *et al.*, Eur. Phys. J. D **58**, 1 (2010).

[2] N. Sangouard, C. Simon, H. de Riedmatten, and N. Gisin, Rev. Mod. Phys. **83**, 33 (2011).

[3] F. Bussieres, N. Sangouard, M. Afzelius, H. de Riedmatten, C. Simon, and W. Tittel, J. Mod. Opt. **60**, 1519 (2013).

[4] T. E. Northup and R. Blatt, Nat. Photonics **8**, 356 (2014).

[5] K. Heshami, D. G. England, P. C. Humphreys, P. J. Bustard, V. M. Acosta, J. Nunn, and B. J. Sussman, J. Mod. Opt. **63**, 2005 (2016).

[6] S. Wehner, D. Elkouss, and R. Hanson, Science **362**, eaam9288 (2018).

[7] C. W. Chow, J. Laurat, H. Deng, K. S. Choi, H. de Riedmatten, D. Felinto, and H. J. Kimble, Science **316**, 1316 (2007).

[8] S. Ritter, C. Nolleke, C. Hahn, A. Reiserer, A. Neuzner, M. Uphoff, M. Mucke, E. Figueroa, J. Bochmann, and G. Rempe, Nature (London) **484**, 195 (2012).

[9] H. Bernien, B. Hensen, W. Pfaff, G. Koolstra, M. S. Blok, L. Robledo, T. H. Taminiau, M. Markham, D. J. Twitchen, L. Childress, and R. Hanson, Nature (London) **497**, 86 (2013).

[10] W. B. Gao, P. Fallahi, E. Togan, J. Miguel-Sanchez, and A. Imamoglu, Nature (London) **491**, 426 (2012).

[11] K. De Greve, L. Yu, P. L. McMahon, J. S. Pelc, C. M. Natarajan, N. Y. Kim, E. Abe, S. Maier, C. Schneider, M. Kamp, S. Hofling, R. H. Hadfield, A. Forchel, M. M. Fejer, and Y. Yamamoto, Nature (London) **491**, 421 (2012).

[12] H. de Riedmatten, M. Afzelius, M. U. Staudt, C. Simon, and N. Gisin, Nature (London) **456**, 773 (2008).

[13] M. Zhong, M. P. Hedges, R. L. Ahlefeldt, J. G. Bartholomew, S. E. Beavan, S. M. Wittig, J. J. Longdell, and M. J. Sellars, Nature (London) **517**, 177 (2015).

[14] C. Clausen, I. Usmani, F. Bussieres, N. Sangouard, M. Afzelius, H. de Riedmatten, and N. Gisin, Nature (London) **469**, 508 (2011).

[15] E. Saglamyurek, N. Sinclair, J. Jin, J. A. Slater, D. Oblak, F. Bussieres, M. George, R. Ricken, W. Sohler, and W. Tittel, Nature (London) **469**, 512 (2011).

[16] C. Clausen, F. Bussieres, M. Afzelius, and N. Gisin, Phys. Rev. Lett. **108**, 190503 (2012).

[17] M. Gundogan, P. M. Ledingham, A. Almasi, M. Cristiani, and H. de Riedmatten, Phys. Rev. Lett. **108**, 190504 (2012).

[18] Z. Q. Zhou, W. B. Lin, M. Yang, C. F. Li, and G. C. Guo, Phys. Rev. Lett. **108**, 190505 (2012).

[19] Z. Q. Zhou, Y. L. Hua, X. Liu, G. Chen, J. S. Xu, Y. J. Han, C. F. Li, and G. C. Guo, Phys. Rev. Lett. **115**, 070502 (2015).

[20] M. Afzelius, C. Simon, H. de Riedmatten, and N. Gisin, Phys. Rev. A **79**, 052329 (2009).

[21] P. Jobez, C. Laplane, N. Timoney, N. Gisin, A. Ferrier, P. Goldner, and M. Afzelius, Phys. Rev. Lett. **114**, 230502 (2015).

[22] M. Gundogan, P. M. Ledingham, K. Kutluer, M. Mazzera, and H. de Riedmatten, Phys. Rev. Lett. **114**, 230501 (2015).

[23] A. Seri, A. Lenhard, D. Rielander, M. Gundogan, P. M. Ledingham, M. Mazzera, and H. de Riedmatten, Phys. Rev. X **7**, 021028 (2017).

[24] A. Tiranov, P. C. Strassmann, J. Lavoie, N. Brunner, M. Huber, V. B. Verma, S. W. Nam, R. P. Mirin, A. E. Lita, F. Marsili, M. Afzelius, F. Bussieres, and N. Gisin, Phys. Rev. Lett. **117**, 240506 (2016).

[25] N. Sinclair, E. Saglamyurek, H. Mallahzadeh, J. A. Slater, M. George, R. Ricken, M. P. Hedges, D. Oblak, C. Simon, W. Sohler, and W. Tittel, Phys. Rev. Lett. **113**, 053603 (2014).

[26] A. Seri, D. Lago-Rivera, A. Lenhard, G. Corrielli, R. Osellame, M. Mazzera, and H. de Riedmatten, Phys. Rev. Lett. **123**, 080502 (2019).

[27] D. Guery-Odelin, A. Ruschhaupt, A. Kiely, E. Torrontegui, S. Martinez-Garaot, and J. G. Muga, Rev. Mod. Phys. **91**, 045001 (2019).

[28] X. Chen, I. Lizuain, A. Ruschhaupt, D. Guery-Odelin, and J. G. Muga, Phys. Rev. Lett. **105**, 123003 (2010).

[29] M. G. Bason, M. Viteau, N. Malossi, P. Huillery, E. Arimondo, D. Ciampini, R. Fazio, V. Giovannetti, R. Mannella, and O. Morsch, Nat. Phys. **8**, 147 (2012).

[30] J. Zhang, J. H. Shim, I. Niemeyer, T. Taniguchi, T. Teraji, H. Abe, S. Onoda, T. Yamamoto, T. Ohshima, J. Isoya, and D. Suter, Phys. Rev. Lett. **110**, 240501 (2013).

[31] G. T. Genov, M. Hain, N. V. Vitanov, and T. Halfmann, Phys. Rev. A **101**, 013827 (2020).

[32] B. T. Torosov, S. Guerin, and N. V. Vitanov, Phys. Rev. Lett. **106**, 233001 (2011).

[33] G. T. Genov, D. Schraft, T. Halfmann, and N. V. Vitanov, Phys. Rev. Lett. **113**, 043001 (2014).

[34] G. T. Genov and N. V. Vitanov, Phys. Rev. Lett. **110**, 133002 (2013).

[35] A. Baksic, H. Ribeiro, and A. A. Clerk, Phys. Rev. Lett. **116**, 230503 (2016).

[36] B. B. Zhou, A. Baksic, H. Ribeiro, C. G. Yale, F. J. Heremans, P. C. Jerger, A. Auer, G. Burkard, A. A. Clerk, and D. D. Awschalom, Nat. Phys. **13**, 330 (2017).

[37] J. Minář, N. Sangouard, M. Afzelius, H. de Riedmatten, and N. Gisin, Phys. Rev. A **82**, 042309 (2010).

[38] S. N. Shevchenko, S. Ashhab, and F. Nori, Phys. Rep. **492**, 1 (2010).

[39] C. W. Thiel, T. Bottger, and R. L. Cone, J. Lumin. **131**, 353 (2011).

[40] H. Ribeiro, G. Burkard, J. R. Petta, H. Lu, and A. C. Gossard, Phys. Rev. Lett. **110**, 086804 (2013).

[41] L. M. Duan, M. D. Lukin, J. I. Cirac, and P. Zoller, Nature (London) **414**, 413 (2001).

[42] D. F. Phillips, A. Fleischhauer, A. Mair, R. L. Walsworth, and M. D. Lukin, Phys. Rev. Lett. **86**, 783 (2001).

[43] M. P. Hedges, J. J. Longdell, Y. Li, and M. J. Sellars, Nature (London) **465**, 1052 (2010).

[44] B. Julsgaard, C. Grezes, P. Bertet, and K. Molmer, Phys. Rev. Lett. **110**, 250503 (2013).

[45] G. Kurizki, P. Bertet, Y. Kubo, K. Molmer, D. Petrosyan, P. Rabl, and J. Schmiedmayer, Proc. Natl. Acad. Sci. USA **112**, 3866 (2015).